

Hybrid Nanocomposites: Advanced Nonlinear Method for Calculating Key Kinetic Parameters of Complex Cure Kinetics

Camille Alzina, Nicolas Sbirrazzuoli, and Alice Mija*

Thermokinetic Group, Laboratory of Chemistry of Organic and Metallic Materials C.M.O.M., University of Nice — Sophia Antipolis, 06108 Nice Cedex 2, France

Received: May 4, 2010; Revised Manuscript Received: July 22, 2010

Complex cure kinetics involved in the elaboration of organic/inorganic hybrid silicate nanocomposites based on diglycidyl ether of bisphenol A (DGEBA), 1,3-phenylenediamine (*m*-PDA), and modified montmorillonite (MMTm) clay have been studied. An advanced isoconversional method has been applied to nonisothermal data in order to evaluate cure kinetic parameters. A new method based on nonlinear optimization was proposed to compute nonisothermal kinetic parameters avoiding complex optimization techniques. The objective is to obtain kinetic parameters rather than modeling values in order to give more insight into the elucidation of complex cure mechanisms. Key kinetic parameters of cure have been computed according to this method. It appears that the reaction mechanism changes if MMTm is added to the curing system. The results reveal an increase of the efficiency of collisions in presence of MMTm at the beginning of the cure and an increase of the frequency of diffusion jumps at the later stage of the reaction.

1. Introduction

Epoxy resins provide excellent mechanical and thermal properties and are often used as polymer matrices for composites and, more recently, for nanocomposites. In this latter area, the size reduction of fillers may lead to a set of new physicochemical properties, rich in potential applications such as improved barrier and bactericidal properties, resistance to fire, or enhancement of mechanical properties. Layered silicate nanocomposites are widely studied in recent years.^{1–11}

The cross-linking reaction between epoxy resins (DGEBA) with diamine curing agent (*m*-PDA) is a complex mechanism composed by four chemical reactions (primary amine–epoxy, secondary amine–epoxy, etherification, and homopolymerization) and two physical phenomena (gelation and vitrification) that occur during cure. The incorporation of modified montmorillonite (MMTm) can catalyze the epoxy–amine polymerization (including polyaddition, etherification, and homopolymerization) reactions¹² and change the kinetics parameters of cure.

The kinetic calculations are often performed to provide the parameters that best describe the experimental data. The beginning of the polymerization of an epoxy resin with a primary amine corresponds to an autocatalyzed step. In the literature, two models are employed: Kamal and Sourour and Kamal.

Sourour and Kamal¹³ developed a two-step autocatalytic cure model:

$$\frac{d\alpha}{dt} = [k_1(T) + k_2(T)\alpha](1 - \alpha)(B - \alpha) \quad (1)$$

Here $k_1(T)$ represents the rate coefficient of amine addition initiated by a proton donor HX, $k_2(T)$ is the rate coefficient of amine catalyzed by the presence of hydroxyl group formed

during the first stage, and B equals 1 for a stoichiometric mixture of an epoxy monomer with an initiator. A simple transformation

$$\frac{d\alpha/dt}{(1 - \alpha)^2} = k_1(T) + k_2(T)\alpha \quad (2)$$

allows for the evaluation of the rate coefficients as parameters of a linear regression which usually holds up to $\alpha = 0.3–0.4$.¹³ The left side of eq 2 is often called the reduced reaction rate. Then, the rate coefficients $k_1(T)$ and $k_2(T)$ can be determined for different temperatures and used to evaluate Arrhenius parameters A_1 , E_1 , A_2 , and E_2 , which correspond respectively to the rate coefficients $k_1(T)$ and $k_2(T)$. The results obtained using this computation for the DGEBA/*m*-PDA system were presented in a previous study.¹⁴

This method was not often used in nonisothermal mode because computational problems can arise by simultaneously varying T and α in eq 2. In order to avoid this problem, isothermal cuts of nonisothermal DSC data can be used to apply eq 2, leading to a relatively complex procedure.¹⁵

A more general autocatalytic model was proposed by Kamal:¹⁶

$$\frac{d\alpha}{dt} = [k_1(T) + k_2(T)\alpha^m](1 - \alpha)^n \quad (3)$$

Several numerical procedures have been suggested^{17–19} for fitting data of eq 3. Model fitting is facilitated by setting constraints on the values of m and n . It is usually assumed that $m + n$ equals 2^{20,16,17,21} but not always.^{22–28}

Many works have been presented to adjust the parameters considering either isothermal,^{15,20,29–36,14} nonisothermal,^{15,37–39} or both isothermal and nonisothermal data,⁴⁰ but the physical meaning of these parameters is not clear. According to Perrin et al.,³⁰ m and n are adjustable power exponents which have definite physical meaning in very limiting cases. Lopez et al.³⁸

* To whom correspondence should be addressed. E-mail: mija@unice.fr.

report that the parameters found with the Sourour and Kamal model do not have any physical meaning. Hernandez-Ortiz et al.⁴¹ highlighted that in the proposed fitting methods some parameters values cannot be always interpreted physically. In this numerical procedure 18 parameters were computed simultaneously. Kamal's model has been widely used to describe complex kinetic cures and is widely used in modeling software for industry. Nevertheless, obtaining meaningful parameters by fitting Kamal's model is still a challenge because if too many parameters are computed simultaneously, computational problems associated with excessive uncertainty in the parameters arise.

As an alternative, we propose a new method to determine nonisothermal kinetic parameters of complex cures. This method uses the E_α dependency obtained by a model-free isoconversional kinetic treatment of nonisothermal DSC data, and then nonlinear fitting of the dependency is used to compute the parameters of the Kamal model. Note that any other kinetic model could be used instead of Kamal's model, if appropriate. As the degree of freedom of the system is considerably reduced, because the nonlinear fit is applied to the E_α dependency and not to crude nonisothermal data, we expect to obtain kinetic parameters rather than modeling values. During the past decade, many studies have shown that analysis of this dependency is physically sounded.⁴² The same procedure has also been applied to the end of reaction using a diffusion model. The goal of this study is to give more insight into the elucidation of complex cure mechanisms involved in the synthesis of organic/inorganic hybrid silicates nanocomposites. The obtained parameters will be analyzed by comparing the values of the curing of an epoxy-based polymer and of an epoxy-layered silicate nanocomposite in regard to the difference in the possible chemical mechanisms of the two systems.

2. Experimental Part

2.1. Materials. Na⁺-montmorillonite (Optigel EX0255, subsequently called MMT) with a cationic exchange capacity (CEC) of about 100 mequiv/100 g was obtained from Süd Chemie. Octadecylamine, 1,3-phenylenediamine (*m*-PDA), and diglycidyl ether of bisphenol A (DGEBA) were obtained from Sigma-Aldrich and used as received. DGEBA has a molecular weight of about 355 g mol⁻¹, a glass transition temperature T_g of about -20 °C (midpoint DSC), and an epoxy equivalent (determined by ¹H NMR) of about 175 g equiv⁻¹.

2.2. Samples Preparation. Organically modified montmorillonite (subsequently called MMTm) was prepared using a method described in the literature.⁴³ Epoxy and clay were mixed in proportion of 95/5 (w/w) using a Bioblock 20 kHz–750 W sonifier fitted with a 3 mm titanium probe (2 times 10 min, 50% pulse, intensity 38%). Further, a stoichiometric amount of curing agent, *m*-PDA, was added and mixed for ~5 min at 70 °C.

Two kinds of samples were prepared: DGEBA/*m*-PDA and DGEBA/MMTm/*m*-PDA. The mixtures were stored below the glass transition temperature of the unreacted material ($T_{g,0}$) at -30 °C for no more than 2 days. Cross-linking reactions were directly performed in DSC aluminum pans by simple heating.

2.3. Experimental Techniques. Differential scanning calorimetry (DSC) measurements were carried out on a Mettler-Toledo DSC 823°. The apparatus is equipped with a HSS7 ceramic sensor (heat-flux sensor with 2 × 120 thermocouples Au–Au/Pd), which allows very high sensitivity. Temperature and enthalpy calibrations were performed by using indium and zinc standards. Integrations of DSC peaks were done using a

line type of baseline. Samples of about 10 mg were placed in 40 μL aluminum crucibles. The different mixtures were cured under nonisothermal conditions at 1, 2, 3, and 4 °C min⁻¹.

2.4. Evaluation of Kinetic Parameters. The general equation of the reaction rate for heterogeneous condensed phase reactions is written as⁴⁴

$$\frac{d\alpha}{dt} = k(T)f(\alpha) \quad (4)$$

where $k(T)$ is the Arrhenius rate coefficient, t is the time, T is the temperature, $f(\alpha)$ is the reaction model that represents the mechanism of a process, and α is the extent of conversion. Introducing the Arrhenius equation

$$k(T) = A \exp\left(\frac{-E}{RT}\right) \quad (5)$$

where E is the activation energy, A is the pre-exponential factor, and R is the gas constant, eq 4 becomes

$$\frac{d\alpha}{dt} = A \exp\left(\frac{-E}{RT}\right)f(\alpha) \quad (6)$$

2.4.1. Nonisothermal Kinetic Methods. 2.4.1.1. *Borchardt–Daniels's and Achar–Brindley–Sharp's Differential Methods.* The differential methods of Borchardt–Daniels⁴⁵ or Achar–Brindley–Sharp (ABS)⁴⁶ are obtained by taking the logarithm of eq 6:

$$\ln\left(\frac{d\alpha}{dt}\right) - \ln f(\alpha) = \ln A - \frac{E}{RT} \quad (7)$$

The left side of eq 7 can be evaluated for several reaction models $f(\alpha)$.⁴⁷ The discrimination between various mathematical models is achieved using statistical criteria, usually the correlation coefficient of the plot of the left-hand side of eq 7 vs $1/T$ (slope $-E/R$ and intercept $\ln A$). This approach was often used for solid-state chemistry, but Vyazovkin et al.^{48–50} have shown that the differences observed between several mechanisms for nonisothermal data is not necessarily significant from statistical point of view.

In the computational method proposed in this work, the discrimination between various mathematical models is not achieved. The ABS equation is simply used to compute compensation parameters, as explained in the following section.

Compensation Effect. The “compensation effect” observed when a model-fitting method is applied to a single heating rate run can be used to determine $\ln A_\alpha$ for each value of α .^{51,52} The method is based on the experimental observations that the same calorimetric curve can be described by several reaction models.^{53–55} The Arrhenius parameters E and $\ln A$ were computed using the differential model-fitting method of Achar–Brindley–Sharp (ABS) for each reaction models (0.20 < α < 0.80). Using the apparent compensation effect that exists when the model changes, the compensation parameters a and b are determined according to

$$\ln A_i = aE_i + b \quad (8)$$

where a and b are constants and the subscript i refers to a factor producing a change in the Arrhenius parameters. This factor

can be conversion, heating rate, or reaction model (as in this work). Then, the compensation parameters of eq 8 are used to compute a value of $\ln A_\alpha$ for each value of E_α . In the present work, this method was used to give estimations for the initial values of $\ln A$ in order to compute kinetic parameters using a nonlinear minimization method (Solver Microsoft Excel).

2.4.1.2. Isoconversional Methods. Isoconversional methods are based on the isoconversional principle, stating that the reaction rate at constant extent of conversion is only a function of temperature.⁴² According to eq 4

$$\left[\frac{d \ln(d\alpha/dt)}{dT^{-1}} \right]_\alpha = \left[\frac{d \ln k(T)}{dT^{-1}} \right]_\alpha + \left[\frac{d \ln f(\alpha)}{dT^{-1}} \right]_\alpha \quad (9)$$

Henceforth, the subscript α indicates the values related to a given extent of conversion. Because $f(\alpha)$ does not depend on T , when α is constant, hence

$$\left[\frac{d \ln(d\alpha/dt)}{dT^{-1}} \right]_\alpha = -\frac{E_\alpha}{R} \quad (10)$$

As can be seen from eq 10, a completely model-free value of E can be estimated for each α value.

2.4.1.3. Advanced Nonlinear Integral Isoconversional Vyazovkin Method (NLN). The E_α dependency is computed according to the advanced isoconversional method proposed by Vyazovkin.^{56,57} This method is based on a direct numerical integration of eq 6. According to this method, for a set of n experiments carried out at different arbitrary heating programs $T_i(t)$, the activation energy is determined at any particular value of α by finding the value of E_α that minimizes the function

$$\Phi(E_\alpha) = \sum_{i=1}^n \sum_{j \neq i}^n \frac{J[E_\alpha, T_i(t_\alpha)]}{J[E_\alpha, T_j(t_\alpha)]} \quad (11)$$

In eq 11 the integral

$$J[E_\alpha, T_i(t_\alpha)] = \int_{t_\alpha - \Delta\alpha}^{t_\alpha} \exp\left[\frac{-E_\alpha}{RT_i(t)}\right] dt \quad (12)$$

is evaluated numerically, using the trapezoidal rule, for a set of experimental heating programs. Integration is performed over small time segments (eq 12) and allows to eliminate the systematic errors occurring in the usual integral methods when E_α varies significantly with α . In eq 12, α is varied from $\Delta\alpha$ to $1 - \Delta\alpha$ with a step $\Delta\alpha = m^{-1}$, where m is the number of intervals chosen for analysis.⁵⁷ This last method is often called the nonlinear isoconversional method (NLN), or advanced isoconversional method, or Vyazovkin method.

All these kinetic methods were programmed using a software already described.^{58,59} For all these methods, the minimization procedure is repeated for each 0.01 α value ($0.01 < \alpha < 0.99$).

We have demonstrated that the application of the isoconversional method (eqs 11 and 12) to incomplete isothermal cures causes a systematic error in the E_α dependency, if one uses the absolute values of α .⁶⁰ The error can be eliminated by using the α values related to the relative extent of cure. Then, the resulting dependency should be reassigned to the absolute extent of cure, if desired. Recently, Sbirrazzuoli has demonstrated⁶¹

that the Vyazovkin method can be applied to transformations with temperature-dependent reaction heat, as is the case of epoxy cures.

2.4.2. Nonisothermal Kinetic Treatment Applied to Curing Reactions. **2.4.2.1. Kinetically Controlled Cure.** Both isothermal and nonisothermal fitting procedures present their drawbacks, but a good fitting of experimental data, in the chemically controlled part of the reaction, is generally obtained using these methods. Nevertheless, obtaining meaningful kinetic parameters is not straightforward because too many parameters have to be evaluated simultaneously in the nonisothermal fitting procedure.

As an alternative, we propose to compute the parameters of the Kamal model using the E_α dependency obtained after treatment of nonisothermal DSC data. In this case, the mathematical expression of the reaction rate is given by eq 3.

Equation 10 can be used to evaluate the kinetic parameters describing the cure kinetics from the E_α dependency. For this, the isoconversional principle is applied introducing eq 3 into eq 10:

$$E_\alpha = \frac{k_1(T)E_1 + k_2(T)E_2\alpha^m}{k_1(T) + k_2(T)\alpha^m} \quad (13)$$

Introducing $k_1(T) = A_1 \exp(-E_1/RT)$ and $k_2(T) = A_2 \exp(-E_2/RT)$, eq 13 leads to eq 14

$$E_\alpha = \frac{(A_1/A_2) \exp(-E_1/RT)E_1 + \exp(-E_2/RT)E_2\alpha^m}{(A_1/A_2) \exp(-E_1/RT) + \exp(-E_2/RT)\alpha^m} \equiv E_\alpha(T) \quad (14)$$

In order to compute a value of the pre-exponential factor for each value of E estimated by advanced isoconversional method (eqs 11 and 12), we used the apparent compensatory effect (eq 8) existing between $\ln A$ and E when the model changes.

Using the advanced isoconversional method, E_α is computed for various α values, lying between 0.01 and 0.99. The E_α dependency can be easily converted to a dependency of E_α on T . This is accomplished by considering the average of the temperatures corresponding to a given α for the various heating rates used in the computation. The resulting temperature dependency $E_\alpha(T)$ was used to compute the kinetic parameters A_1/A_2 , E_1 , E_2 , and m , using a nonlinear minimization method applied to eq 14.

One of the advantages of this method is that it provides a way for estimate the starting values of E and $\ln A$ used in the minimization procedure.

2.4.2.2. Diffusion-Controlled Cure. In the case of chemical reactions controlled by diffusion of oligomers,^{14,55,62,63} the characteristic decrease of the effective activation energy E_α can be rationalized in terms of a kinetic model^{64,65} for a process occurring in a mixed diffusion-kinetic regime:^{14,66,67}

$$k_{\text{ef}}^{-1} = k^{-1}(T) + k_D^{-1}(T, \alpha) \quad (15)$$

where k_{ef} , $k(T)$, and $k_D(T, \alpha)$ are the effective, reaction, and diffusion rate coefficients, respectively.

Equation 16 has already been proposed for the expression of $k_D(T, \alpha)$.⁶²

$$k_D(T, \alpha) = D_0 \exp(-E_D/RT + K\alpha) \quad (16)$$

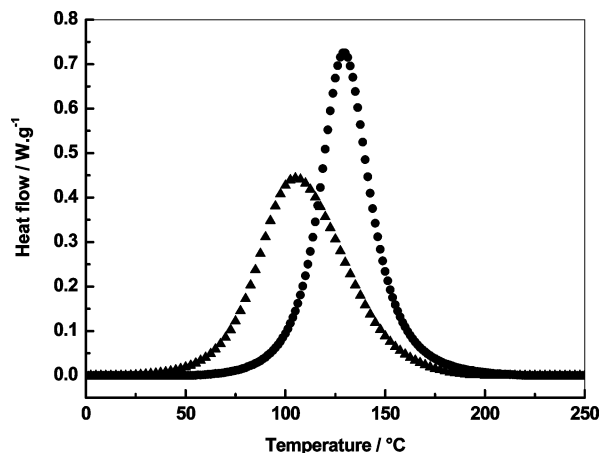


Figure 1. DSC data of the heat release during nonisothermal cures of the DGEBA/*m*-PDA (circles) and DGEBA/MMTm/*m*-PDA (triangles) mixtures at 3 °C min⁻¹.

where K is a constant accounting for the effect of the chemical reaction on the change in diffusivity, D_0 is the pre-exponential factor, and E_D is the activation energy of diffusion. The usual Arrhenius expression was used for $k(T) = A \exp(-E/RT)$, where A is the pre-exponential factor and E is the activation energy of the chemical reaction. According to this model, the experimentally measured effective activation energy, E_{ef} , is a function of the activation energies of both chemical reaction and diffusion. Applying the isoconversional principle to eqs 10 and 15

$$E_{ef} = -R \left(\frac{d \ln k_{ef}}{dT^{-1}} \right)_{\alpha} = \frac{k(T)E_D + k_D(T, \alpha)E}{k(T) + k_D(T, \alpha)} \quad (17)$$

Here E_{ef} is a function of the temperature and $E_{ef} = E_{ef}(T)$. The dependency of E_{α} on α may be written as $E_{\alpha} = E_{ef}(T_{\alpha})$, i.e., by substituting the temperatures related to given conversions into eq 17 when computing the values of k and k_D . Equation 17 can also be transformed into eq 18:

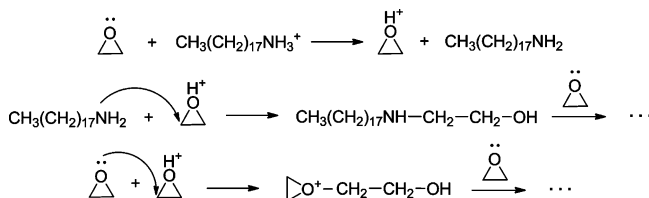
$$E_{\alpha} = \frac{(A/D_0) \exp(-E/RT)E_D + \exp(-E_D/RT + K\alpha)E}{(A/D_0)A \exp(-E/RT) + \exp(-E_D/RT + K\alpha)} \equiv E_{ef}(T_{\alpha}) \quad (18)$$

This method allows for the computation of the Arrhenius parameters, A/D_0 , E , E_D , and K , simultaneously, using a nonlinear minimization algorithm applied to eq 18.

3. Results and Discussion

3.1. Kinetic Results Obtained by Advanced Isoconversional Method. The various stoichiometric mixtures DGEBA/*m*-PDA and DGEBA/MMTm/*m*-PDA were cured under nonisothermal conditions. The DSC curves obtained at 3 °C min⁻¹ are represented in Figure 1. As seen in Figure 1, the presence of MMTm in the DGEBA/*m*-PDA curing system shifts the reaction to lower temperature. In addition, a change of the shape of the thermoanalytical curve can also be noticed. This suggests a possible modification of the cure mechanism and so of the kinetic parameters in the presence of MMTm. This shift can be explained by the effect of the primary ammonium cations NH₃⁺ of the MMTm which act as epoxy ring-opening initiator due to the release of a proton H⁺, producing an oxonium ion and a

SCHEME 1: Polymerization Initiated by CH₃(CH₂)₁₇NH₃⁺ of MMTm



primary amine (Scheme 1). The generated CH₃(CH₂)₁₇NH₂ specie may react with an epoxy group, entering in competition with the *m*-PDA curing agent. Then, the epoxy ring can react with the oxonium ion to form ether links.

The E_{α} dependencies were evaluated using the advanced isoconversional method of eqs 11 and 12 from DSC data (Figure 1). The results are presented in Figure 2a,b. The compensation parameters of eq 8 were used to compute a value of $\ln A_{\alpha}$ for each value of E_{α} as presented in Figure 2a. We found $a = 0.3190 \text{ mol kJ}^{-1}$, $b = -7.8479$, and $r^2 = 0.9991$.

We can note that the two systems have not the same E_{α} dependency. A previous publication⁶⁸ indicates that the first stage of the dependency of DGEBA/*m*-PDA is characteristic of epoxy-amine reactions. At the end of the reaction, the decrease to a value as low as $\sim 10 \text{ kJ mol}^{-1}$ is due to the transition from chemical control of the cross-linking to a diffusion control that becomes detectable in this system already at gelation.⁶⁸ In the case of DGEBA/MMTm/*m*-PDA system, the characteristic decrease of E_{α} observed when $\alpha \rightarrow 1$ is lower, leading to the hypothesis that diffusion contribution is less pronounced in this case. This can be explained by a higher molecular mobility. Side reactions (etherifications/homopolymerizations) are known to occur at elevated temperatures, so it can also be postulated that these reactions become significant at a lower temperature in the case of DGEBA/MMTm/*m*-PDA.¹⁴ In fact, these two phenomena are linked because side reactions are reactivated when the molecular mobility of the viscous media increases, i.e., when the system devitrifies.

As the presence of MMTm in the DGEBA/*m*-PDA system shift the reaction to lower temperatures (Figure 1), we have calculated the E_{α} dependency of the two systems as a function of temperature (mean temperature over the heating rates) as shown in Figure 2b. These data show a very good agreement of the dependencies of the two systems at the middle stage of the reaction, i.e., between 90 °C < T < 130 °C. The main differences between the two systems are observed at the initial and final cure stages. For the DGEBA/MMTm/*m*-PDA system, the characteristic decrease of E_{α} reported for catalytic effect⁶² is greater, in agreement with the hypothesis of an easier ring-opening in the presence of MMTm. According to Figure 2a, the apparent activation energy vs conversion is always higher for the system with MMTm. In fact, the additional information obtained by plotting E_{α} vs T of Figure 2b indicates that the apparent activation energy values are higher for the system DGEBA/MMTm/*m*-PDA at lower temperature, where the reaction of the system DGEBA/*m*-PDA is negligible. Thus, these higher E_{α} values correspond to the reactions initiated by MMTm (Scheme 1). Because the two chemical reactions do not occur in the same temperature interval, the conversion degrees are not related to a same reaction temperature.

3.2. Fitting of the E_{α} Dependency Using the Two-Step Autocatalytic Model. A nonlinear procedure based on the minimization of the sum of the square of the residuals was applied to eq 14, for a conversion interval ranging between 0.03

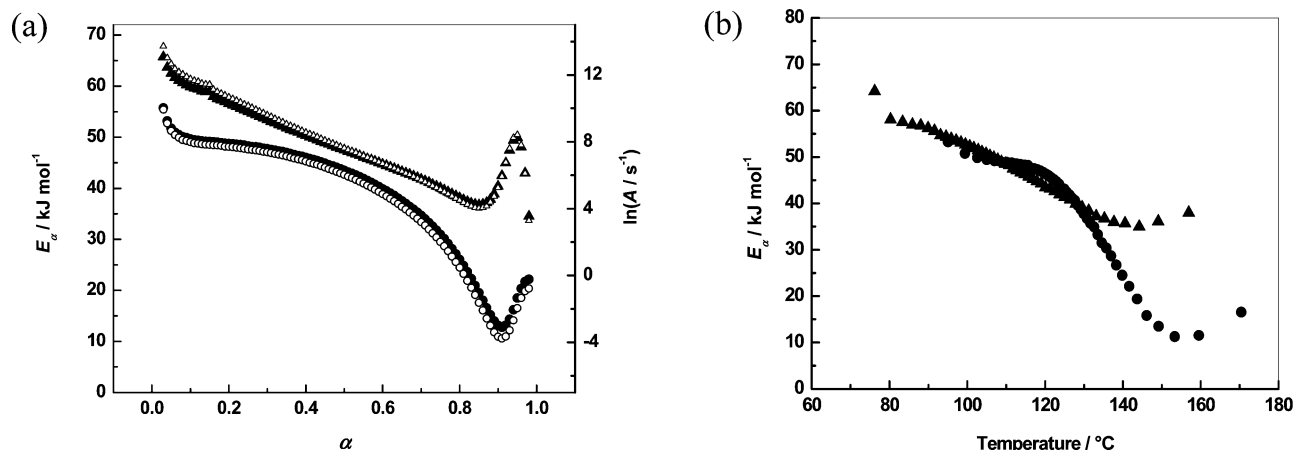


Figure 2. Isoconversional computations: (a) E_α and $\ln A_\alpha$ dependencies; (b) E_α vs T dependencies. Circles: DGEBA/*m*-PDA system; triangles: DGEBA/MMTm/*m*-PDA system (open: $\ln A_\alpha$ dependency; solid: E_α dependency).

TABLE 1: Kinetic Parameters Obtained from Two-Step Autocatalytic Model after Nonlinear Minimization Applied to Eq 14

	A_1/A_2	$E_1/\text{kJ mol}^{-1}$	$E_2/\text{kJ mol}^{-1}$	m
DGEBA/ <i>m</i> -PDA	41.54	69.77	45.24	1.11
DGEBA/MMTm/ <i>m</i> -PDA	88.83	75.92	52.94	1.10

$< \alpha < 0.15$. This interval was chosen because it corresponds to the very beginning of the cure, which is known to be chemically controlled and which has been frequently described using a two-step autocatalytic model. The initial values of A_1 and A_2 introduced in the nonlinear minimization method applied to eq 14 were computed using eq 8 that gives the existing relation between $\ln A$ and E .

According to eq 8 and to the NLN method, a value of $\ln A_\alpha$ was computed for each α . The initial values of E_1 and E_2 were taken as the values of E_{ef} for $\alpha = 0.03$ and $\alpha = 0.15$, respectively (E_α -dependency presented in Figure 2a). The initial value for m was $m = 1$. Table 1 gives the kinetic parameters obtained after nonlinear minimization using eq 14 for $0.03 < \alpha < 0.15$. Curve fitting using eq 14 is presented in Figure 3.

For the DGEBA/*m*-PDA system, the activation energy E_1 of the amine addition initiated by a proton donor, $E_1 \sim 70 \text{ kJ mol}^{-1}$, is slightly higher than the activation energy of the amine addition catalyzed by the presence of hydroxyl group formed during the first stage, $E_2 \sim 45 \text{ kJ mol}^{-1}$. This is in good agreement with a previous work,¹⁴ where the Sourour and Kamal model of eq 2

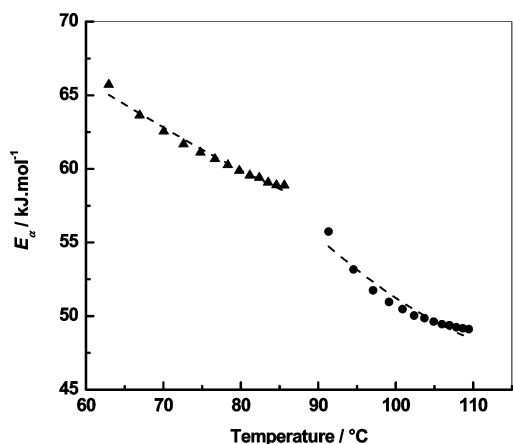


Figure 3. Experimental and fitted data (dash) of $E_\alpha(T)$ dependencies using the two-step autocatalytic model after nonlinear minimization; DGEBA/*m*-PDA: circles; DGEBA/MMTm/*m*-PDA: triangles.

was used to estimate E_1 and E_2 for isothermal curing DGEBA/*m*-PDA. The activation energy E_1 was found to be greater than the activation energy E_2 . The same trend is observed for the DGEBA/MMTm/*m*-PDA system.

This result was also obtained for TGDDM/DDS epoxy-amine systems from isothermal experiments.^{27,28} The values of m determined in these last two publications were closed to one (no constraint was applied). In our case, the values of m presented in Table 1 are very similar and close to one. These values are close to the initial starting value used in the minimization procedure ($m = 1$).

The values of A_1/A_2 , E_1 , and E_2 are always higher for the system containing MMTm (Table 1), suggesting a change in the reaction mechanism. Because the kinetic parameters are directly linked to the shape of the thermoanalytical curves, it can also be postulated looking at Figure 1 that the reactions mechanism may changes when MMTm is added to the system.

According to the two-step autocatalytic model proposed by Kamal,¹⁶ the activation energies E_1 and E_2 are slightly higher in presence of MMTm. Nevertheless, the difference is low. This can seem contradictory with the fact that the reaction is shifted to lower temperatures. Reminding that E and $\ln A$ have opposite effects in regard to the shift vs temperature, this suggests an increase of the pre-exponential factor in the presence of MMTm because an increase of the pre-exponential factor shifts the reaction to lower temperatures. This hypothesis is in perfect agreement with the results shown in Figure 2 (values of $\ln A$).

Additional information can be extracted from Table 1. The pre-exponential factor ratio A_1/A_2 is clearly higher for the DGEBA/MMTm/*m*-PDA system. In the presence of MMTm, amine addition initiated by a proton donor (Scheme 1) is facilitated. We can therefore speculate that the value A_1 for the system with MMTm is higher than the value A_1 for reference system while the values of A_2 for the two systems show little change or A_1 and A_2 change simultaneously in various ratios. Thus, we can postulate that addition of MMTm increases the efficiency of collisions. This hypothesis was proposed by Vyazovkin⁶⁹ and accepted by Li et al.^{70,71} which show that the reactivity of a system under nanoconstraints is modified due to an enhancement of effective collisions.

This has been explained by a higher difficulty of the molecules to diffuse apart because of the high surface area of MMTm and the enhancement of chemical reactions because of the presence of a nearby surface.

Equation 1 can be easily transformed into eq 14':

$$E_{\alpha} = \frac{A_1 \exp(-E_1/RT)E_1 + A_2 \exp(-E_2/RT)E_2\alpha^m}{A_1 \exp(-E_1/RT) + A_2 \exp(-E_2/RT)\alpha^m} \equiv E_{\alpha}(T) \quad (14')$$

The same nonlinear procedure, with constraint $(A_1/A_2) = 41.54$ and $(A_1/A_2) = 88.83$ (Table 1), has been applied to this latter equation to compute the parameters A_1 and A_2 . The values obtained are $A_1 = 20739.16 \text{ s}^{-1}$, $A_2 = 499.23 \text{ s}^{-1}$ for the DGEBA/*m*-PDA system and $A_1 = 6599126.31 \text{ s}^{-1}$, $A_2 = 74291.61 \text{ s}^{-1}$ for the DGEBA/MMTm/*m*-PDA system. In perfect agreement with the previously mentioned qualitative hypotheses, this computation confirms that A_1 and A_2 are higher in the presence of MMTm. A_1 is 318 times higher and A_2 149 times when MMTm is added. Thus, addition of MMTm induces a high modification of efficiency of collisions of the amine addition initiated by a proton donor that result in an enhancement of the ring opening.

Equation 14 does not allow the evaluation of the kinetic exponent n , but it is generally supposed a second-order reaction or $m + n = 2$.^{20,16,17,21} Indeed, calculations were performed on isothermal data for epoxy resins, and the error between the predicted values of the rate and those obtained from the data were found to be the lowest when the value of $m + n$ was about 2.^{20,72}

We proposed here another method of determination of n (without constraint) based on the application of eq 3 for a given extent of conversion. For this, eq 3 can be transformed in eq 19

$$\left[\frac{d\alpha}{dt(1-\alpha)^n} \right]_{\alpha} = k_1(T_{\alpha}) + k_2(T_{\alpha})\alpha^m \quad (19)$$

where T_{α} is the temperature related to a given extent of conversion and $[d\alpha/dt(1-\alpha)^n]_{\alpha}$ is the reduced reaction rate related to a given extent of conversion. The results are presented in Table 2. As can be seen in Table 2, m is higher in the presence of MMTm, in good agreement with the hypothesis of a change in the reaction mechanism. Because octadecylamine is formed (Scheme 1), the system with clay becomes nonstoichiometric, leading to a higher value of m for the DGEBA/MMTm/*m*-PDA system. The reaction mechanism is more complex in the case of DGEBA/MMTm/*m*-PDA system, and this is reflected on the value of the kinetic exponent n . This value is higher in the presence of MMTm compared to the reference without MMTm.

3.3. Fitting of the E_{α} Dependency Using the Diffusion Model. A similar nonlinear minimization procedure was applied to eq 18. The nonlinear fit was applied for a conversion interval ranging between $0.30 < \alpha < 0.85$. This interval was chosen because it corresponds to the extent of conversion where diffusion becomes significant.^{64,68} The initial values of $\ln A$ and $\ln D_0$ were selected using the same procedure as previously described. The initial values of E and E_D have been respectively taken as value of E_{ef} for $\alpha = 0.30$ and $\alpha = 0.85$ from the E_{α} dependency presented in Figure 2a. Table 3 gives the results obtained after the nonlinear minimization, using eq 18 for $0.30 < \alpha < 0.85$, and Figure 4 gives the fit of the E_{α} dependency using these parameters.

The kinetic parameters K , E , and E_D obtained in Table 3 are higher in the presence of MMTm. The activation energy of the chemically controlled reaction E obtained for DGEBA/*m*-PDA and DGEBA/MMTm/*m*-PDA systems are close each other and also very close to those obtained in Table 1 for the autocatalyzed

TABLE 2: Two-Step Autocatalytic Model^a

	m	n	$m + n$	r^2
DGEBA/ <i>m</i> -PDA	0.51	1.86	2.37	0.9950
DGEBA/MMTm/ <i>m</i> -PDA	0.66	1.92	2.58	0.9968

^a m and n are kinetic values after minimization applied to eq 19.

TABLE 3: Kinetic Parameters Obtained from Diffusion Model after Nonlinear Minimization Applied to Eq 18

	A/D_0	K	$E/\text{kJ mol}^{-1}$	$E_D/\text{kJ mol}^{-1}$
DGEBA/ <i>m</i> -PDA	1234.58	-7.06	47.71	4.41
DGEBA/MMTm/ <i>m</i> -PDA	9.66	-5.88	53.47	34.12

reaction E_2 of DGEBA/*m*-PDA and DGEBA/MMTm/*m*-PDA systems, respectively. For the two systems, the activation energy of the chemically controlled reaction E is very close to the model-free value previously obtained for the primary amine/epoxy addition.⁶⁸

It has been shown previously⁶² that the high decrease of the apparent activation energy observed at the end of the reaction can be attributed to a change from a chemically controlled reaction to a diffusion-controlled regime. Thus, the low value observed for E_D is characteristic to the diffusion of oligomers in the glassy state. According to this, it can be concluded that the diffusion control is reduced when MMTm is added, in agreement with the higher value of E_D reported in Table 3.

The ratios A/D_0 reported in Table 3 show a different tendency. The value obtained for the nanocomposite DGEBA/MMTm/*m*-PDA is lower. Several hypotheses can be formulated, and separate conclusions on each parameter are difficult to formulate. In order to obtain more information on the variation of these two parameters, eq 18 has been transformed into eq 18':

$$E_{\alpha} = \frac{A \exp(-E/RT)E_D + D_0 \exp(-E_D/RT + K\alpha)E}{A \exp(-E/RT) + D_0 \exp(-E_D/RT + K\alpha)} \equiv E_{\text{ef}}(T_{\alpha}) \quad (18')$$

Then, the same nonlinear procedure, with constraint $(A/D_0) = 1234.59$ and $(A/D_0) = 9.66$ (Table 3), have been applied to this latter equation to compute the parameters A and D_0 . The resulting values are $A = 1762.24 \text{ s}^{-1}$, $D_0 = 1.43 \text{ s}^{-1}$ for DGEBA/*m*-PDA and $A = 13\,777.00 \text{ s}^{-1}$, $D_0 = 1426.76 \text{ s}^{-1}$ for DGEBA/MMTm/*m*-PDA. These values show that both A and D_0 are

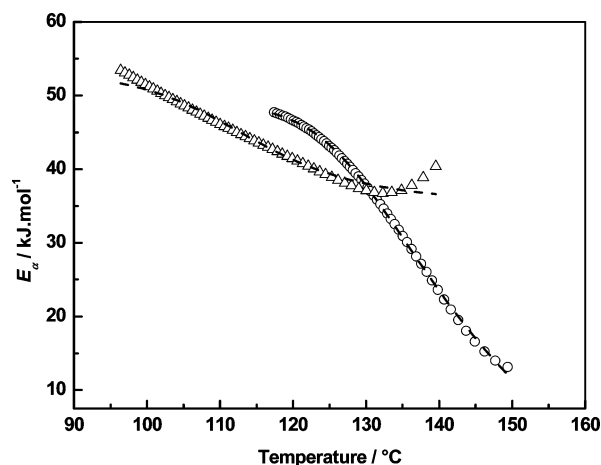


Figure 4. Experimental and fitted data (dash) of $E_{\alpha}(T)$ dependencies using the diffusion model after nonlinear minimization. DGEBA/*m*-PDA: circles; DGEBA/MMTm/*m*-PDA: triangles.

higher in the presence of MMTm, but the ratio A/D_0 is lower for the nanocomposite DGEBA/MMTm/*m*-PDA. For the nanocomposite, A is about 8 times higher, while D_0 is about 1000 times higher.

In the presence of clay, the cross-linking density is lower because of the formation of ether links; thus, the molecular mobility is higher and T_g is lower. As stated,⁷³ the characteristic time of the jump (k_d^{-1}) can be approximated by the relaxation time (τ) because diffusion occurs as a succession of molecular jumps between the neighboring equilibrium positions, so that we can write

$$k_d^{-1} \approx \tau = \frac{4\pi a^3 \eta}{kT} \quad (20)$$

where η is the viscosity of the medium, a is the molecular radius, k is Boltzmann's constant, and T is the absolute temperature. Thus, a lower cross-link density and T_g mean that at the same temperature the viscosity is lower; i.e., τ is smaller, and the frequency of diffusion jumps D_0 is higher.

The values obtained for the parameter K (Table 3) also support this statement. Addition of MMTm leads to an increase of K . K is a constant accounting for the effect of the chemical reaction on the change in diffusivity. In eq 16, the term $K\alpha$ is opposite in sign to that of the term E/RT . A lower K value decreases the numerical value of the reaction coefficient $k_p(T, \alpha)$, for a same value of D_0 , because the term $\exp(-E/RT + K\alpha)$ decreases.

The final stages of the reaction ($0.30 < \alpha < 0.85$) show a complex behavior. The logarithm of rate coefficients $k(T)$ and $k_p(T)$ can be computed for the final stages of the reaction according to the value of Table 3. $k(T)$ is always slightly higher with MMTm, while for a same value of the temperature, the diffusion rate coefficient $k_p(T)$ is lower. Because $k(T)$ is higher for the nanocomposite, it can be concluded that the chemical reactions have more facility to occur at the end of the reaction in presence of MMTm.

4. Conclusions

This paper proposes a new method to obtain nonisothermal kinetic parameters of complex reactions. Thus, this method was applied for the determination of pre-exponential factors and elucidation of cure kinetics involved in the elaboration of organic/inorganic hybrid silicate nanocomposites.

Kinetic parameters and the E_α dependencies were computed with an advanced isoconversional method. It was found that the mechanism changes when organically modified clay is added to the curing system. This appears by a shift of the chemical reactions to lower temperature and a change of the shape of the thermoanalytical curves. The obtained values of kinetic parameters of cure in the presence of clay are modified for the nanocomposite. This results in different E_α dependencies for the two systems, suggesting a modification of the cure mechanism. The primary ammonium cations NH_3^+ of the modified clay acts as an epoxy ring-opening initiator so the generated species may react with epoxy groups, entering in competition with the curing agent. Addition of modified clay induces less ineffective shocks, and the reactivity is modified due to an enhancement of efficiency of collisions. For the chemically controlled part of the reaction, the high increase of the efficiency of collisions of the amine addition initiated by a proton donor results in an enhancement of the ring-opening. In the diffusion controlled part of the reaction, the pre-exponential factor is also

increased by addition of modified clay and was explained by a high increase of the frequency of diffusion jumps (1000 times).

Acknowledgment. The authors acknowledge the PACA region and the company SICOMIN Composites for financial support.

References and Notes

- (1) Pavlidou, S.; Papaspyrides, C. D. *Prog. Polym. Sci.* **2008**, *33*, 1119.
- (2) Ray, S. S.; Okamoto, M. *Prog. Polym. Sci.* **2003**, *28*, 1539.
- (3) Alexandre, M.; Dubois, P. *Mater. Sci. Eng.* **2000**, *28*, 1.
- (4) Okada, A.; Usuki, A. *Macromol. Mater. Eng.* **2006**, *291*, 1449.
- (5) De Paiva, L. B.; Morales, A. R.; Díaz, F. R. V. *Appl. Clay Sci.* **2008**, *42*, 8.
- (6) Lan, T.; Pinnavaia, T. J. *Chem. Mater.* **1994**, *6*, 2216.
- (7) Ngo, T.-D.; Ton-That, M.-T.; Hoa, S. V.; Cole, K. C. *J. Appl. Polym. Sci.* **2008**, *107*, 1154.
- (8) Zhang, K.; Wang, L.; Wang, F.; Wang, G.; Li, Z. *J. Appl. Polym. Sci.* **2004**, *91*, 2649.
- (9) Dean, K.; Krstina, J.; Tian, W.; Varley, R. J. *Macromol. Mater. Eng.* **2007**, *292*, 415.
- (10) Guo, B.; Jia, D.; Cai, C. *Eur. Polym. J.* **2004**, *40*, 1743.
- (11) Salahuddin, N. *Polym. Adv. Technol.* **2004**, *15*, 251.
- (12) Lan, T.; Kviratna, P. D.; Pinnavaia, T. J. *Chem. Mater.* **1995**, *7*, 2144.
- (13) Sourour, S.; Kamal, M. R. *Thermochim. Acta* **1976**, *14*, 41.
- (14) Sbirrazzuoli, N.; Mititelu-Mija, A.; Vincent, L.; Alzina, C. *Thermochim. Acta* **2006**, *447*, 167.
- (15) Vyazovkin, S.; Sbirrazzuoli, N. *Macromol. Chem. Phys.* **1999**, *200* (10), 2294.
- (16) Kamal, M. R. *Polym. Eng. Sci.* **1974**, *14*, 231.
- (17) Ryan, M. E.; Dutta, A. *Polymer* **1979**, *20*, 203.
- (18) Min, B.-G.; Strachunski, Z. H.; Hodgkin, J. H. *Polymer* **1993**, *34*, 4488.
- (19) Kenny, J. M. *J. Appl. Polym. Sci.* **1994**, *51*, 761.
- (20) Mijovic, J.; Kim, J.; Slaby, J. *J. Appl. Polym. Sci.* **1984**, *29*, 1449.
- (21) Foun, C. C.; Moroni, A.; Pearce, E. M.; Mijovic, J. *Polym. Mater. Sci. Eng.* **1984**, *51*, 411.
- (22) Su, C. C.; Woo, E. M. *Polymer* **1995**, *36*, 2883.
- (23) Hsieh, H. K.; Su, C. C.; Woo, E. M. *Polymer* **1998**, *39*, 2175.
- (24) Su, C. C.; Woo, E. M.; Huang, Y. P. *Polym. Eng. Sci.* **2005**, *45* (1), 1.
- (25) Liu, Y.; Zhao, M.; Shen, S.; Gao, J. *J. Appl. Polym. Sci.* **1998**, *70*, 1991.
- (26) Han, S.; Kim, W. G.; Yoon, H. G.; Moon, T. J. *J. Polym. Sci., Part A* **1998**, *36*, 773.
- (27) Xie, H.; Liu, B.; Sun, Q.; Yuan, Z.; Shen, J.; Cheng, R. *J. Appl. Polym. Sci.* **2005**, *96*, 329.
- (28) Lopez, J.; Lopez-Bueno, I.; Nogueira, P.; Ramirez, C.; Abad, M. J.; Barral, L.; Cano, J. *Polymer* **2001**, *42*, 1669.
- (29) Mijovic, J. *J. Appl. Polym. Sci.* **1986**, *31*, 1177.
- (30) Perrin, F. X.; Nguyen, T. M. H.; Vernet, J. L. *Eur. Polym. J.* **2007**, *43*, 5107.
- (31) Atarsia, A.; Boukhili, R. *Polym. Eng. Sci.* **2000**, *40*, 3.
- (32) Bae, J.; Jang, J.; Yoon, S.-H. *Macromol. Chem. Phys.* **2002**, *203* (15), 2196.
- (33) Barral, L.; Cano, J.; Lopez, A. J.; Lopez, J.; Nogueira, P.; Ramirez, C. *J. Appl. Polym. Sci.* **1995**, *56*, 1029.
- (34) Min, B.-G.; Stachurski, Z. H.; Hodgkin, J. H. *Polymer* **1993**, *34* (21), 448.
- (35) Lahlali, D.; Naffakh, M.; Dumon, M. *Polym. Eng. Sci.* **2005**, *45* (12), 1581.
- (36) Ramírez, C.; Rico, M.; Torres, A.; Barral, L.; López, J.; Montero, B. *Eur. Polym. J.* **2008**, *44*, 3035.
- (37) Spoelstra, A. B.; Peters, G. W. M.; Meijer, H. E. H. *Polym. Eng. Sci.* **1996**, *36* (16), 2153.
- (38) Lopez, L. M.; Cosgrove, A. B.; Hernandez-Ortiz, J. P.; Osswald, T. A. *Polym. Eng. Sci.* **2007**, *47* (5), 675.
- (39) Hernandez-Ortiz, J. P.; Osswald, T. A. *J. Polym. Eng.* **2005**, *25* (1), 23.
- (40) Van Assche, G.; Van Hemelrijck, A.; Rahier, H.; Van Mele, B. *Thermochim. Acta* **1996**, *286*, 209.
- (41) Hernandez-Ortiz, J. P.; Osswald, T. A. *J. Polym. Eng.* **2005**, *25* (1), 23.
- (42) Vyazovkin, S.; Sbirrazzuoli, N. *Macromol. Rapid Commun.* **2006**, *27*, 1515.
- (43) Le Pluart, L.; Duchet, J.; Sautereau, H.; Gérard, J. F. *J. Adhes.* **2002**, *78*, 645.
- (44) Prime, R. B. *Thermosets*. In *Thermal Characterization of Polymeric Materials*, 2nd ed.; Turi, E. A., Ed.; Academic Press: New York, 1997; p 1380.

- (45) Borchardt, H. J.; Daniels, F. *J. Am. Chem. Soc.* **1957**, *79*, 41.
- (46) Achar, B. B.; Brindley, G. W.; Sharp, J. H. *Proc. Int. Clay Conf. Jerusalem*; Heller & Weiss: 1966; Vol. 1, p 67.
- (47) Brown, M. E.; Dollimore, D.; Galwey, A. K. *Reactions in the Solid State. Comprehensive Chemical Kinetics*; Amsterdam: Elsevier, 1980; Vol. 22.
- (48) Vyazovkin, S.; Lesnikovich, A. I. *J. Therm. Anal.* **1985**, *30*, 831.
- (49) Vyazovkin, S.; Lesnikovich, A. I. *J. Therm. Anal.* **1987**, *32*, 249.
- (50) Vyazovkin, S.; Lesnikovich, A. I. *Thermochim. Acta* **1990**, *165*, 11.
- (51) Vyazovkin, S.; Lesnikovich, A. I. *Thermochim. Acta* **1988**, *128*, 297.
- (52) Vyazovkin, S. *Int. J. Chem. Kinet.* **1996**, *28*, 95.
- (53) Vyazovkin, S.; Linert, W. *Chem. Phys.* **1995**, *193*, 109.
- (54) Budrugaec, P.; Segal, E. *Polym. Degrad. Stab.* **2008**, *93*, 1073.
- (55) Cadenato, A.; Moranco, J. M.; Fernández-Francos, X.; Salla, J. M.; Ramis, X. *J. Therm. Anal. Calorim.* **2007**, *89*, 233.
- (56) Vyazovkin, S. *J. Comput. Chem.* **1997**, *18* (3), 393.
- (57) Vyazovkin, S. *J. Comput. Chem.* **2001**, *22*, 178.
- (58) Sbirrazzuoli, N.; Brunel, D.; Elégant, L. *J. Therm. Anal. Calorim.* **1992**, *38* (6), 1509.
- (59) Sbirrazzuoli, N. *Macromol. Chem. Phys.* **2007**, *208*, 1592.
- (60) Vyazovkin, S.; Sbirrazzuoli, N. *Macromol. Rapid Commun.* **2002**, *21* (2), 85.
- (61) Sbirrazzuoli, N. *Macromol. Chem. Phys.* **2007**, *208*, 1592.
- (62) Vyazovkin, S.; Sbirrazzuoli, N. *Macromolecules* **1996**, *29* (6), 1867.
- (63) Guigo, N.; Mija, A.; Vincent, L.; Sbirrazzuoli, N. *Phys. Chem. Chem. Phys.* **2007**, *9* (39), 5359.
- (64) Frank-Kamenetskii, D. A. *Diffusion and Heat Transfer in Chemical Kinetics*, 2nd ed.; Plenum Press: New York, 1969.
- (65) Rabinowitch, E. *Trans. Faraday Soc.* **1937**, *33*, 1225.
- (66) Stutz, H.; Mertes, J.; Neubecker, K. *J. Polym. Sci., Part A* **1993**, *31*, 1879.
- (67) Vyazovkin, S.; Mititelu, A.; Sbirrazzuoli, N. *Macromol. Rapid Commun.* **2003**, *24* (18), 1060.
- (68) Sbirrazzuoli, N.; Vyazovkin, S.; Mititelu, A.; Sladic, C.; Vincent, L. *Macromol. Chem. Phys.* **2003**, *204* (15), 1815.
- (69) Private communication with Professor Sergey Vyazovkin from University of Alabama at Birmingham.
- (70) Li, Q. X.; Simon, S. L. *Macromolecules* **2008**, *41*, 1310.
- (71) Li, Q. X.; Simon, S. L. *Macromolecules* **2009**, *42*, 3573.
- (72) Lee, S. N.; Chiu, M. T.; Lin, H. S. *Polym. Eng. Sci.* **1992**, *32* (15), 1037.
- (73) Vyazovkin, S.; Sbirrazzuoli, N. *Macromol. Chem. Phys.* **2000**, *201*, 199.

JP1040629